



ELSEVIER

Available online at www.sciencedirect.com

SCIENCE @ DIRECT®

Proceedings of the Combustion Institute xxx (2004) xxx–xxx

Proceedings
 of the
Combustion
Institute
www.elsevier.com/locate/proci

Investigations of the scaling criteria for a mild combustion burner

Sudarshan Kumar, P.J. Paul*, H.S. Mukunda

*Combustion Gasification and Propulsion Laboratory, Department of Aerospace Engineering,
 Indian Institute of Science, Bangalore 560 012, India*

8 Abstract

9 In this paper, a new strategy for scaling burners based on “mild combustion” is evolved and adopted to
 10 scaling a burner from 3 to a 150 kW burner at a high heat release rate of 5 MW/m³. Existing scaling meth-
 11 ods (constant velocity, constant residence time, and Cole’s procedure [Proc. Combust. Inst., 28 (2000)
 12 1297]) are found to be inadequate for mild combustion burners; Constant velocity approach leads to
 13 reduced heat release rates at large sizes and constant residence time approach in unacceptable levels of
 14 pressure drop across the system. To achieve mild combustion at high heat release rates at all scales, a mod-
 15 ified approach with high recirculation is adopted in the present studies. Major geometrical dimensions are
 16 scaled as $D \sim Q^{1/3}$ with an air injection velocity of ~ 100 m/s ($\Delta p \sim 600$ mm water gauge). Using CFD sup-
 17 port, the position of air injection holes is selected to enhance the recirculation rates. The precise role of
 18 secondary air is to increase the recirculation rates and burn up the residual CO in the downstream. Mea-
 19 sures involving temperature and oxidizer concentrations inside 3 kW, 150 kW burner and a jet flame are
 20 used to distinguish the combustion process in these burners. The burner can be used for a wide range of
 21 fuels from LPG to producer gas as extremes. Up to 8 dB of noise level reduction is observed in comparison
 22 to the conventional combustion mode. Exhaust NO emissions below 26 and 3 ppm and temperatures 1710
 23 and 1520 K were measured for LPG and producer gas when the burner is operated at stoichiometry.

24 © 2004 by the Combustion Institute. Published by Elsevier Inc. All rights reserved.

25 *Keywords:* Flameless combustion; Mild combustion; Burner scaling; NO_x emissions

27 1. Introduction

28 Guidelines for scaling are important in the de-
 29 sign of combustion systems. A large number of
 30 dimensionless groups for scaling are proposed by
 31 Spalding [1] and Beer and Chigier [2]. It is recog-
 32 nized that maintaining all the variables constant
 33 during the process is not possible partly because
 34 of internal inconsistencies. It is imperative to

adapt scaling based on a selected set of non-di- 35
 36 mensional quantities.

37 Constant velocity, CV and constant residence 38
 39 time, CRT approaches have been applied to scale 40
 41 up the burners and furnaces from laboratory scale 42
 43 [3–10]. For a burner, the total thermal input is gi- 44
 45 ven as $Q = \dot{m}_f H = K \rho U_o D_o^2$. In CV approach, the 46
 47 burner inlet velocity is maintained constant, and 48
 48 geometrical dimensions are derived from the rela-
 49 tionship $D_2/D_1 = (Q_2/Q_1)^{1/2}$. For CRT approach,
 50 the ratio D_o/U_o (inertial or convective timescale)
 51 is maintained constant while increasing the burner
 52 thermal input. The new physical dimensions are
 53 determined through a relationship $D_2/D_1 = (Q_2/$

* Corresponding author. Fax: +91 80 236 016 92.
 E-mail address: paul@cgpl.iisc.ernet.in (P.J. Paul).

Nomenclature		Producer gas	Low calorific value gas (H ₂ ~ 20%, CO ~ 20%, CH ₄ ~ 2%, CO ₂ ~ 13% and rest N ₂)
CRT	Constant residence time scaling approach	Q, Q_1, Q_2	Burner thermal input (kW)
CV	Constant velocity scaling approach	U_o, U_a, U_f	Inlet velocity of air/fuel or characteristic velocity (m/s)
$D, D_o,$ D_1, D_2	Different burner dimensions	\dot{m}_a, \dot{m}_f	Air and fuel flow rates
f_v	Volume fraction	\dot{Q}'''	Heat release rate per unit volume MW /m ³
H	Calorific value of fuel	ρ	Density of air/fuel (kg/m ³)
LPG	Liquefied petroleum gas (~80% butane and 20% propane)	$\tau_{\text{mixing}}, \tau_a, \tau_f$	Characteristic mixing time or convective timescales, D_o/U_o (μs)

49 $Q_1)^{1/3}$. In another approach adopted by Cole et al.
50 [8], both air velocity and jet area are increased
51 equally for scaling combustors. The velocity and
52 jet diameters are scaled as $U_2/U_1 = (Q_2/Q_1)^{1/2}$ and
53 $D_2/D_1 = (Q_2/Q_1)^{1/4}$ to burner inputs. More details
54 about the variation of critical parameters with dif-
55 ferent scaling approaches are given in Table 1.

56 It is known that CV approach increases the
57 characteristic mixing time and reduces the rate
58 of mixing [3–10]. To maintain constant rate of
59 mixing, the inlet velocity should be increased as
60 $Q^{1/3}$ with burner thermal input [4–6,8]. In Cole's
61 [8] approach, jet velocity increases at faster rate
62 than jet diameter. Therefore, both CRT and
63 Cole's [8] approaches lead to large pressure drop
64 across the combustion system. The experimental
65 investigations using Cole's [8] approach on an
66 acoustically excited combustor showed consistent
67 performance for pollutant emissions, flame stabil-

ity, and enhanced mixing at smaller levels. The
68 improvement in emissions' performance at larger
69 power scales is reported to be insignificant. 70

71 The scaling studies on swirl stabilized pulverized
72 coal burners have shown that NO_x emissions dep-
73 end on local fluid flow behavior in the internal
74 recirculation zone [4,5]. Computational investiga-
75 tions by Weber and Breussin [6] predicted that be-
76 yond a certain thermal input, NO_x emissions
77 remained independent of the scaling approach
78 used.

79 CV approach fails to produce aerodynamic sim-
80 ilarity in the near burner region for swirl stabilized
81 natural gas burners [7]. This is a critical factor for
82 NO_x formation in the gas burners. Detailed analy-
83 sis of NO_x emissions from two gas burners at 67 and
84 266 kW thermal levels showed the importance of
85 prompt NO formation in the near burner zone of
86 a combustion system [10].

Table 1
Comparison of various parameters in different scaling approaches

Scaling approaches	Geometric scaling $D = (D_2/D_1)$	Velocity scaling $U = (U_2/U_1)$	τ_{mixing}	Re	\dot{Q}'''
CV	$\sim Q^{1/2}$	Constant	$\sim Q^{1/2}$	$\sim Q^{1/2}$	$\sim Q^{1/2}$
CRT	$\sim Q^{1/3}$	$\sim Q^{1/3}$	Constant	$\sim Q^{2/3}$	Constant
Cole [9]	$\sim Q^{1/4}$	$\sim Q^{1/2}$	$\sim Q^{-1/4}$	$\sim Q^{3/4}$	$\sim Q^{1/4}$
Present	$\sim Q^{1/3}$	~ 100 m/s	$\sim Q^{1/3}$	$\sim Q^{1/3}$	Constant

Table 2
Summary of the previous work in mild combustion and residence times used in these experiments

Ref.	U_f (m/s)	τ_f (μs)	U_a (m/s)	τ_a (μs)	\dot{Q}''' (MW/m ³)	\dot{Q} (kW)
[12]	20	250	73.7	74.6	0.32	10
[13]	9.34	503.2	33	151.51	0.18	6
[14]	12.57	318.21	28.9	162.58	0.18	6
[18]	100	100	70	1771	0.023	580
[20]	7.9–70.7	114–4.2	—	—	—	—
[15]	20–100	25–5	26–130	77–15.5	5.6	1–5
Present	243	3	95	52	5.6	150

87 The exhaust gas recirculation for NO_x reduction
 88 from combustion systems has drawn interest
 89 due to its promising features [11–16]. When recirculation
 90 rates are high enough and at temperatures greater than the
 91 auto-ignition temperature of the fuel, a stable combustion
 92 mode exists. This combustion mode is known as mild or
 93 flameless combustion [11–19]. Table 2 summarizes the work
 94 carried out on mild combustion. Lower convective
 95 timescales seem to be a critical factor to achieve
 96 mild combustion with high \dot{Q}''' ($\sim 5 \text{ MW/m}^3$) and
 97 reactants at ambient temperature. The previous
 98 experiments are conducted in the thermal range
 99 of 1–580 kW with low heat release rates (23–
 100 320 kW/m^3) [12–15].

102 To scale a burner with high \dot{Q}''' , if one uses a
 103 CRT method, jet velocity increases as $Q^{1/3}$ and
 104 hence leads to unacceptable levels of pressure
 105 drop across the system beyond a certain thermal
 106 input range as shown in Table 3. One needs to explore
 107 other alternatives to scale a mild combustion burner
 108 while maintaining the geometric, dynamic, and thermal
 109 similarities.

110 The objectives of the current research are to
 111 use the results of 3 kW laboratory scale burner,
 112 scale it to a large level, in this case 150 kW, establish
 113 mild combustion in a high heat release burner,
 114 and suggest scaling laws for the mild combustors.

115 2. Computations

116 The objectives of the computational studies are
 117 to optimize the burner geometry, to quantify the
 118 recirculation rates and to predict the combustion
 119 and fluid flow behavior of a 150 kW mild combustion
 120 burner. The same code that was used for
 121 3 kW laboratory burner is used here. The details
 122 related to computational strategy, fluid flow, and
 123 combustion modeling of the burner can be found
 124 in Sudarshan et al. [15]. Since the geometry presents
 125 a sixfold symmetry with six alternate fuel
 126 and air injection jet arrangements along the central
 127 axis, one-sixth part of the burner is considered
 128 for the numerical simulation. To obtain grid independent
 129 results, grid resolution studies are carried out
 130 with the number of grid points varying from
 131 100,000 to 1,000,000. The results with respect to

600,000 grid points were within 1% for all meshes
 up to 1,000,000 grid points.

3. Geometry optimization and computational results 134

135 The 3 kW laboratory burner investigated earlier
 136 by Sudarshan et al. [15] is scaled using CV, CRT,
 137 and Cole's [8] scaling principles. Table 3 shows
 138 the detailed dimensions, velocities, and other related
 139 details of the 150 kW scaled burner with different
 140 approaches. The burner is theoretically scaled to
 141 2 MW to show the effect of different approaches
 142 on recirculation rates and heat release

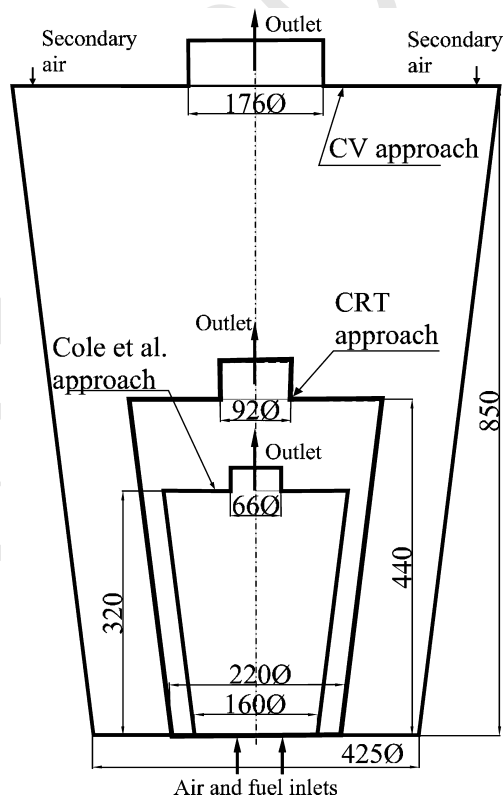


Fig. 1. Details of the 150 kW scaled burner using different approaches.

Table 3

Summary of the geometrical dimensions with different scaling approaches

Scale factor	1	10	50	667
Q (kW)	3	30	150	2000
D_a, U_a for CRT	2, 80	4.3, 172	7.4, 291	17.5, 698
D_1, D_2, L (mm) for CRT	60, 90, 120	130, 194, 258	221, 331, 440	525, 790, 1050
D_1, D_2, L (mm) for CV	60, 90, 120	190, 285, 380	425, 636, 850	1550, 2325, 3100
D_1, D_2, L (mm) Cole [8]	60, 90, 120	107, 160, 214	160, 240, 320	305, 458, 610
Present D_a, U_a	2, 80	—	5, 95	—
Present τ_a (μs)	25	—	52.4	—
Recirculation rate	2.8	—	2.3	—

143 rates. Fig. 1 shows the effect of different scaling ap-
 144 proaches on physical geometry of 150 kW burner.
 145 The physical dimensions of the scaled burner de-
 146 crease from CV to CRT and Cole's [8] approach,
 147 and corresponding \dot{Q}''' increases. Fig. 2 shows the
 148 variation of recirculation rates in 150 kW scaled
 149 burner with different scaling approaches obtained
 150 from computational studies. Curve (a) shows that
 151 the recirculation rates drop from 280% to 220% as
 152 the burner is scaled from 3 kW level to 2 MW using
 153 CRT approach. The air inlet velocity (scaled as
 154 $U_o \sim Q^{1/3}$) increases from 79 to 698 m/s. This leads
 155 to unacceptable level of pressure drop across the
 156 combustion systems. Curve (d) shows that corre-
 157 sponding heat release rate remains constant with
 158 CRT approach. Similarly Cole's [8] ($U_o \sim Q^{1/2}$) ap-
 159 proach also results in large pressure drop across
 160 the combustion systems.

161 When CV scaling approach is used to deter-
 162 mine the burner dimensions, the recirculation
 163 rates drop from 280% to 190% as shown by curve
 164 (b). Curve (e) represents the corresponding \dot{Q}'''
 165 variation with CV approach. The heat release

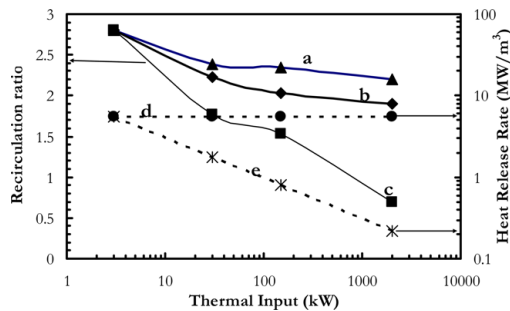


Fig. 2. Variation of recirculation rate and heat release rates with thermal power. Curve (a) Recirculation rate variation with CRT approach. Curve (b) Recirculation rate variation with CV approach. Curve (c) Recirculation rate variation when major burner dimensions are determined through $D \sim Q^{1/3}$ with an air injection velocity of 100 m/s. Curve (d) Variation of heat release rate for CRT approach. Curve (e) Variation of heat release rate for CV approach.

166 rates drastically drop as $1/Q^{1/2}$ from 5.6 to 166
 167 0.217 MW/m^3 as burner is scaled from 3 kW to 167
 168 2 MW. Curve (c) represents variation of recircula- 168
 169 tion rates in the burner when the major burner 169
 170 dimensions are determined to maintain high \dot{Q}''' 170
 171 at 5.6 MW/m^3 and air inlet velocity at $\sim 100 \text{ m/s}$, 171
 172 an affordable choice in industrial applications. 172
 173 To maintain \dot{Q}''' constant, combustion system vol- 173
 174 ume should be increased in proportion to thermal 174
 175 input. Therefore, major burner dimensions are 175
 176 scaled as $D \sim Q^{1/3}$. In the current scaling strategy, 176
 177 recirculation rates drop to 153% at 150 kW and 177
 178 70% at 2 MW level, thus making it difficult to 178
 179 achieve mild combustion in the scaled burners. 179

180 At this point of time, a 150 kW burner scaled 180
 181 from 3 kW laboratory burner is tested experimen- 181
 182 tally for the demonstration of mild combustion 182
 183 mode. The major dimensions are determined 183
 184 using $D \sim Q^{1/3}$ to maintain high \dot{Q}''' . Air jet vel- 184
 185 ocities of 100 m/s are considered. This experimen- 185
 186 tal burner is tested with both LPG and producer gas 186
 187 (typical producer gas composition $\text{CO } 20\%$, H_2 187
 188 20% , CO_2 13% , CH_4 2% , and rest N_2). It is ob- 188
 189 served that due to low recirculation rates and 189
 190 large air and fuel jet diameters (large convective 190
 191 timescales of air and fuel jets), the combustion 191
 192 zones are clearly visible as a kind of highly con- 192
 193 fined jet flames attached to either air or fuel jets 193
 194 (for detailed operating conditions see Table 4). 194
 195 Overall observed emission levels are low. The 195
 196 presence of highly confined jet flames in the com- 196
 197 bustion zone prompted further investigations. 197

198 The steep reduction in recirculation rates led to 198
 199 the exploration of other alternatives to increase 199
 200 the overall recirculation rates to achieve mild 200
 201 combustion. Initial trials with different injection 201
 202 schemes showed that various air/fuel injection 202
 203 schemes had very little effect on overall recircula- 203
 204 tion rates. The air and fuel injection details are 204
 205 shown in Fig. 3. Both air and fuel are injected 205
 206 as a set of six holes at different locations at 206
 207 90 mm pitch diameter. The diameters and number 207
 208 of air and fuel jets are estimated to keep the D_o/U_o 208
 209 ratio in the same range as for laboratory scale 209
 210 burner operational range (see Table 4). The recir- 210
 211 culation rates are further enhanced by appropri- 211

Table 4

Summary of experiments carried out on the mild combustion burners (MC-mild combustion, AF-attached flames, and PG-Producer gas)

Burner	\dot{Q} (kW)	U_f (m/s)	D_f (mm)	τ_f (μs)	U_a (m/s)	D_a (mm)	τ_a (μs)	Fuel	Remarks
I	1	20	0.5	25	27	2	74	LPG	MC
	3	60	0.5	8.3	80	2	25	LPG	MC
	5	100	0.5	5	135	2	14.8	LPG	MC
II	150	125	2	16	100	10	100	LPG	AF
	150	95	12	126	128	10	78	PG	AF
	150	63	6	95	78	5	64	PG	AF
	150	92	5	54	78	5	64	PG	MC
	150	243	0.7	2.9	95	5	52.4	LPG	MC

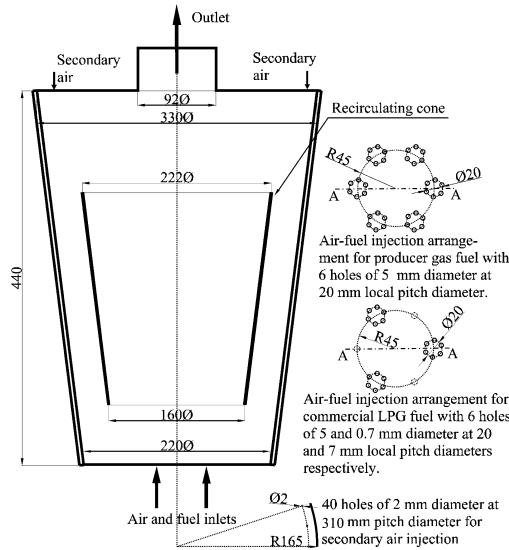


Fig. 3. Details of optimized configuration for 150 kW burner with alternate peripheral injection schemes for both LPG and producer gas fuels.

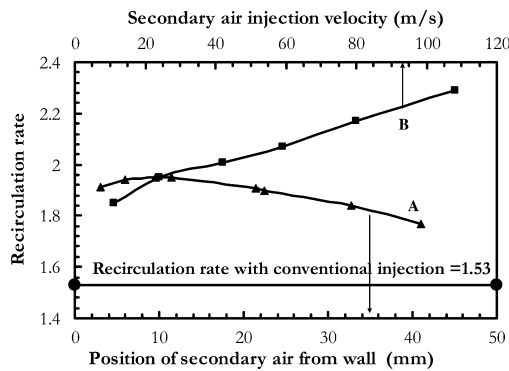


Fig. 4. Variation of recirculation rate with secondary air position and velocity. Curve (A) Variation of recirculation rate with secondary air injection position. Curve (B) Variation of recirculation rate with secondary air velocity at optimum position.

are located at 11 mm from the wall. Curve (b) shows that recirculation rate varies almost linearly with the secondary injection velocity. Compared to the conventionally injected secondary air [15] at 150 kW level, the recirculation rates are enhanced by ~80%.

To establish a quantitative comparison between the burners at different scales, temperature–volume and O₂–volume behavior is extracted from the calculations. The volume elements for $\Delta T = 100$ K and $\Delta X_{O_2} = 0.01$ steps are determined over the entire combustor and plotted for (a) a turbulent jet diffusion flames (b) 150 kW optimized burner, and (c) 3 kW laboratory burner. Figs. 5 and 6 show the cumulative distribution of volume fraction variation with temperature and O₂ for burners at different scales. For a turbulent jet flame, $f_v = 0.54$ for temperature <1000 K and $f_v = 0.54$ for O₂ mass fraction >0.15. For 150 kW optimized burner, $f_v = 0.93$ for temperature >1000 K (auto-ignition temperature of the fuel) and is almost uniformly distributed over the whole range. Similarly, $f_v = 0.96$ for O₂ mass fraction <0.15 and is uniformly distributed in the range of 0–0.15. For a

ately optimizing the position of secondary air injection (~20% of total air). The secondary air is injected as a set of multiple high-speed jets from the top. A number of calculations are carried out to reveal the effect of location and velocity of secondary air injection on recirculation rates. Fig. 4 shows the variation of the recirculation rate with the position of secondary air with respect to the wall and secondary air velocity. Curve (a) shows that the position of secondary jets has a strong effect on the recirculation rate. The recirculation rate reaches a maximum of 196% for a constant injection velocity of 24 m/s when injection holes

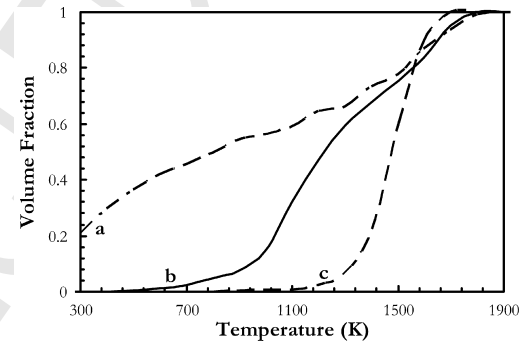


Fig. 5. Predicted cumulative temperature–volume behavior for (a) classical turbulent jet flame. (b) 150 kW scaled burner. (c) 3 kW laboratory scale burner.

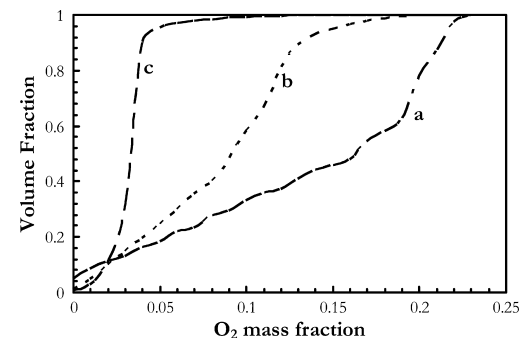


Fig. 6. Predicted cumulative O₂–volume behavior for (a) classical turbulent jet flame. (b) 150 kW scaled burner. (c) 3 kW laboratory scale burner.

249 3 kW mild combustion burner, $f_v = 0.93$ for tem-
250 perature >1300 K and for O_2 mass fraction <0.07 ,
251 $f_v = 0.97$. This deviation of temperature and oxidi-
252 dizer mass fraction distributions from 3 kW mild
253 combustion burner [15] appears significant. This
254 is attributed to the fact that in the current burner,
255 the number of air-fuel jets is six times larger than
256 the previously investigated 3 kW burner. The group
257 of air jets influenced a large volume when compared
258 to a single air jet. For the mild combustion mode,
259 O_2 is typically in the range of 0–0.15, and tempera-
260 ture is greater than 1000 K (auto-ignition tempera-
261 ture of the fuel) [17]. Hence, even case (b) can be
262 considered as in mild combustion mode.

263 4. Scaling of mild combustion burners

264 Table 4 shows the summary of convective time-
265 scales for different combinations of air and fuel
266 jets employed during the experimental investiga-
267 tions. Highly confined, attached, and fluctuating
268 jet flames appeared in the combustion zone below
269 1 kW. The reduction in the air and fuel flow rates
270 leads to reduction in recirculation rates and re-
271 sults in the appearance of attached flames within
272 the reaction zone. At this operating condition,
273 convective timescales for air and fuel jets are 74
274 and 25 μ s, respectively.

275 At 150 kW thermal level, experiments are car-
276 ried out with different air-fuel injection combina-
277 tions for both LPG and producer gas. Highly
278 confined jet flames are observed visibly, attached
279 to either air or fuel jets for the cases of convective
280 timescales greater than ~ 80 μ s. It is observed that
281 mild combustion is obtained successfully with
282 both LPG and producer gas for D_o/U_o ratio below
283 80 μ s. From a series of experiments in the 1–
284 150 kW range on mild combustion burners, it is
285 concluded that for successful scaling of mild combus-
286 tion burners with high heat release rates, $D_o/$
287 U_o ratio should be maintained below ~ 80 μ s.

288 Mild combustion is achieved when flames are
289 lifted off from the primary burner zone at high
290 velocities. This can be explained on the basis of
291 lift-off concept of simple jet diffusion flames,
292 which depends on local temperature, reactant
293 concentration, velocity, and diameter of the injec-
294 tion jets. Confined jet flames are expected to ap-
295 pear in the combustion zone as long the
296 velocities are below blow-off and recirculation
297 rates are low.

298 5. Experiments

299 Two fuels are selected for the experimental
300 studies on 150 kW burner to show that the burner
301 can be used over a wide range of fuels. Producer
302 gas and LPG are chosen as extremes (Calorific val-
303 ue variation 4.5–45 MJ/kg). The burner is oper-

304 ated at stoichiometry with 150 kW thermal 304
305 input. The dimensions of the burner are fixed by 305
306 the total thermal input and \dot{Q}''' in the burner. 306
307 These dimensions are further modified through a 307
308 number of computations aimed at optimizing the 308
309 burner configuration. The details of the air and 309
310 fuel injection schemes for LPG and producer gas 310
311 are shown in Fig. 3. Typical air and LPG mass 311
312 flow rates are 50 and 3.2 g/s. The flow rates for 312
313 producer gas and air are 39 and 47 g/s. Eighty per- 313
314 centage of the total air is supplied through the pri- 314
315 mary inlet and 20% through the secondary inlets. 315
316 The temperatures in the reaction zone are mea- 316
317 sured by using 50 μ m Pt-13%Pt-Rh thermocou- 317
318 ples. Measured temperatures are corrected for 318
319 heat loss by radiation. The corrected temperatures 319
320 are accurate within ± 50 K of actual temperature. 320
321 Species (NO , CO , CO_2 , and O_2) concentrations 321
322 are measured in the reaction zone by using Quintox 322
323 KM-9106 flue gas analyzer. A specially de- 323
324 signed water-cooled stainless steel probe is used 324
325 to draw the sample gases from the reaction zone. 325
326 The sample gases are immediately cooled, dried, 326
327 and then transferred to the analyzer continuously. 327
328 A Lutron SL-4001 sound level meter is used to 328
329 measure the sound levels during the combustion 329
330 experiments. More details of the Quintox gas ana- 330
331 lyzer and sound level meter are mentioned in 331
332 Sudarshan et al. [15]. The noise level measure- 332
333 ments are taken at a point 50 mm from outlet of 333
334 the burner at the same plane. 334

335 6. Results and discussion

336 Most of the results presented in this section are 336
337 for the 150 kW case. The burner is operated at a 337
338 stoichiometric air/fuel ratio. Fig. 7 shows the dis- 338
339 tinction between the conventional combustion 339
340 and mild combustion operation at 150 kW level 340
341 with LPG and producer gas. The conventional 341
342 combustion mode is achieved by reducing the air 342
343 and fuel flow rates in the system leading to lower 343
344 recirculation rates and shifts in operation to at- 344
345 tached flame mode as in Fig. 7A. The burner oper- 345
346 ation in mild combustion mode is shown in Fig. 346
347 7B–D. The injection arrangement is clearly visible 347
348 and totally transparent at the injection plane. A 348
349 very weak flame is present in the reaction zone 349
350 which is light bluish in color and barely visible. 350
351 All the walls are red hot and glowing consistently. 351
352 This combustion mode is achieved by large reci- 352
353 culation rates of the combustion products into 353
354 the fresh reactants. 354

355 The acoustic level measurements are carried 355
356 out during the cold flow (only air jets), mild com- 356
357 bustion mode, and conventional combustion 357
358 mode. The measured levels are 103, 105, and 358
359 113 dB, respectively. Approximately 8 dB of noise 359
360 reduction is observed when operational mode 360
361 shifts from conventional combustion to mild com- 361

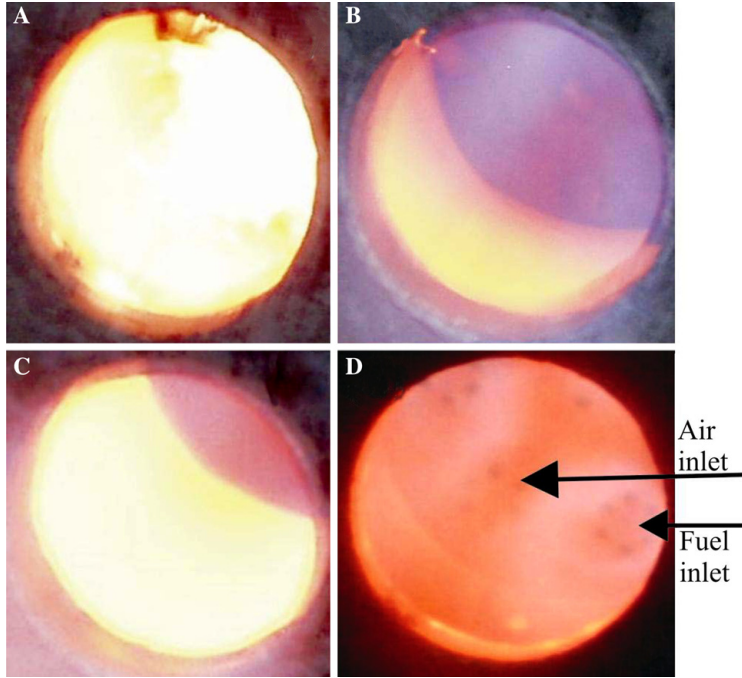


Fig. 7. Comparison between conventional and mild combustion. (A) Conventional turbulent combustion with low recirculation rates. (B,C) Mild combustion mode with LPG fuel. (D) Mild combustion mode with producer gas fuel.

362 bustion for reasons known earlier [15]. Similar
363 noise reduction is observed when the burner is
364 operated with producer gas.

365 The composition of species is measured at two
366 axial locations, 150 and 400 mm downstream
367 from the injection plane. Fig. 8 shows the CO,
368 CO₂, and O₂ mole fractions and temperatures
369 measured at 150 mm axial position across section
370 A–A (Fig. 3). O₂ mole fraction drops from 10% on
371 air jet side to very low values of 1% on fuel jet
372 side. O₂ is fairly well distributed with small gradi-
373 ents across the measuring plane. Measured O₂
374 mole fraction clearly indicates the air and fuel
375 jet injection sides (across section A–A). The spe-
376 cies composition variation across this plane is

377 moderately small. Low species gradients, high
378 temperature, and low concentration of reacting
379 species suggest the presence of a slow reaction
380 over a large area. The measured temperature varies
381 in the range of 1200–1550 K and fairly uniform
382 over the reaction zone.

383 Fig. 9 shows the species and temperature mea-
384 surements 400 mm downstream. The tempera-
385 tures are far more uniform and vary between
386 1500 and 1750 K. The temperature gradients at
387 this plane are much smaller than those compared
388 to 150 mm. The species concentration variation at
389 this plane is very small. The uniformity in species
390 composition across the plane suggests at the con-
391 tinuance of slow combustion reaction at this

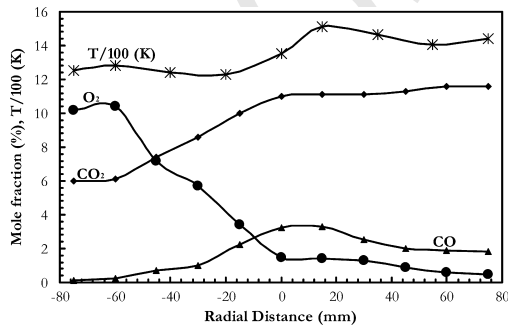


Fig. 8. Species concentration and temperature measurements with LPG fuel at 150 mm from injection plane.

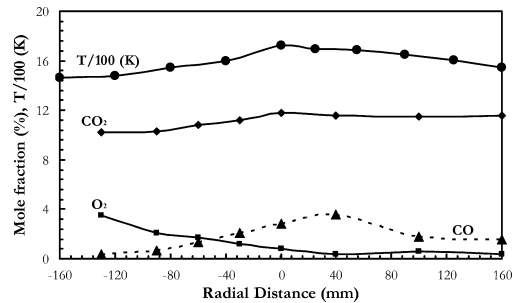


Fig. 9. Species compositions and temperature measurements with LPG fuel at 400 mm from injection plane.

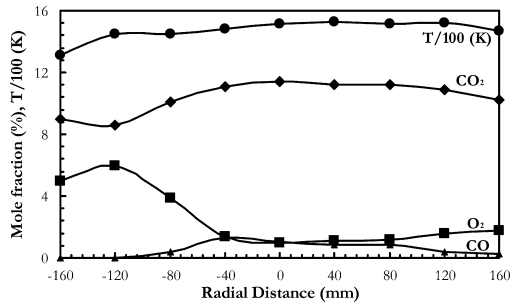


Fig. 10. Species concentration and temperature measurements with producer gas fuel at 400 mm from injection point.

392 plane. At exhaust, the emissions recorded are
 393 26 ppm NO, 1% CO, and an average temperature
 394 1710 K. The CO emissions are in the range of pre-
 395 viously reported experiments [15]. It is observed
 396 during the experiments that very low CO emis-
 397 sions ($\sim 0.03\%$) are recorded when $\sim 10\%$ more
 398 air is added downstream to dilute the combustion
 399 products and burn the residual CO.

400 The injection plane of the burner is slightly
 401 modified to operate the same burner with producer
 402 gas (calorific value ~ 4.5 MJ/kg) as shown in Fig.
 403 3B. The typical stoichiometric ratio for producer
 404 gas is ~ 1.2 . A 200 kW thermal level woody bio-
 405 mass-based gasifier continuously supplied pro-
 406 ducer gas for burner operation [21,22]. Fig. 10
 407 shows the species and temperature measurements
 408 at 400 mm across section A–A. The temperatures
 409 measured at 400 mm are quite uniform across the
 410 radial plane. The important point to note is that
 411 temperature is much more uniform in the reaction
 412 zone than compared to the LPG fuel. Temperature
 413 variations across the radial plane are less than
 414 200 K, and mean temperature is above 1400 K.
 415 The average temperature measured across the ex-
 416 haust plane is 1520 K. Large concentrations of
 417 O₂ on one side and CO on the other side indicate
 418 the approximate position of the air and fuel jets.
 419 Small gradients of CO, CO₂, and O₂ describe the
 420 distributive and sluggish nature of reaction zone
 421 over a large area. Similar behavior of species con-
 422 centration and temperatures are recorded at
 423 150 mm from the injection plane. In contrast to
 424 the LPG operated burner, the NO emissions from
 425 producer gas operation are very low. The measured
 426 CO and NO emissions at the exhaust are 0.211%
 427 and 3 ppm against the 1% and 26 ppm for LPG.
 428 The difference in emissions could be attributed to
 429 a difference in the average operating temperature
 430 (~ 200 K) and in calorific values of two fuels.

431 7. Summary

432 The proposed scaling approach is shown to be
 433 successful in scaling a 3 kW laboratory scale mild

434 combustion burner to 150 kW level. The scaled
 435 burner is operated with two different fuels and
 436 shown to achieve mild combustion at high release
 437 rates (~ 5.6 MW/m³) with both air and fuel at
 438 ambient temperature. The design of its features
 439 has been achieved and optimized through preli-
 440 minary computations, which helped in revealing
 441 the effect of secondary air position and injection
 442 velocity on the recirculation rate. Recirculation
 443 rate is enhanced from 153% to 230% by appropri-
 444 ately positioning the secondary air injection. The
 445 distribution of temperature and O₂ mass fraction
 446 in the combustion chamber is essential in the mild
 447 combustion regime. The cumulative behavior of
 448 temperature–volume and O₂–volume distributions
 449 show that O₂ mass fraction is < 0.15 in 96% of the
 450 total volume, and temperature is > 1000 K in 93%
 451 of the total volume. The presence of low O₂ mass
 452 fraction and high temperature zone in most of the
 453 combustion chamber volume is indicative of mild
 454 combustion at larger power levels with current ap-
 455 proach. Scaling of air and fuel jet combination
 456 based on convective timescales (maintaining be-
 457 low 80 μ s) is an interesting observation. It needs
 458 to be explored further based on simple jet flame
 459 experiments in the similar conditions that exist
 460 in mild combustion burners.

461 The experiments with LPG and producer gas
 462 recorded exhaust emissions of NO below 26 and
 463 3 ppm, respectively. The CO exhaust emissions
 464 observed are 1% and 0.221% with heat release
 465 rates ~ 5.6 MW/m³. The measured temperature
 466 and O₂ gradients in radial direction are moder-
 467 ately small, which implies that combustion is tak-
 468 ing place in mild combustion regime. The
 469 outstanding low chemical emissions, high heat re-
 470 lease rates, operation with two fuels, and low
 471 acoustic emission features strongly indicate the
 472 potential for successful scaling to large power lev-
 473 els and use in industrial furnaces.

474 References

- 475 [1] D.B. Spalding, *Proc. Combust. Inst.* 9 (1962) 833–843.
- 476 [2] J.M. Beer, N.A. Chigier, *Combustion Aerodynamics*, Wiley Press, New York, 1972 (Chapter 7).
- 477 [3] R. Weber, *Proc. Combust. Inst.* 26 (1996) 3343–3354.
- 478 [4] J.P. Smart, D.J. Morgan, P.A. Roberts, *Proc. Combust. Inst.* 24 (1992) 1365–1372.
- 479 [5] J.P. Smart, D.J. Morgan, *Combust. Sci. Technol.* 100 (1994) 331–343.
- 480 [6] R. Weber, F. Breussin, *Proc. Combust. Inst.* 27 (1998) 2957–2964.
- 481 [7] T.C.A. Hsieh, W.J.A. Dahm, J.F. Driscoll, *Combust. Flame*. 114 (1998) 54–80.
- 482 [8] J.A. Cole, T.P. Parr, N.C. Widmer, K.J. Wilson, K.C. Schadow, W.M.R. Seeker, *Proc. Combust. Inst.* 28 (2000) 1297–1304.
- 483 [9] M. Sadakata, Y. Hirose, *Fuel* 73 (8) (1994) 1338–1342.

- 493 [10] A.D. Al-Fawaz, J.T. Dearden, M. Hedley, J.T.
494 Missaghi, M. Pourkashanian, A. Williams, L.T.
495 Yap, *Proc. Combust. Inst.* 25 (1994) 1027–1034.
- 496 [11] J.A. Wunning, J.G. Wunning, *Prog. Energy Com-*
497 *combust. Sci.* 23 (12) (1997) 81–94.
- 498 [12] T. Plessing, N. Peters, J.G. Wunning, *Proc. Com-*
499 *combust. Inst.* 27 (1998) 3197–3204.
- 500 [13] B. Ozdemir, N. Peters, *Exper. Fluids* 30 (2001) 683–
501 695.
- 502 [14] P.J. Coelho, N. Peters, *Combust. Flame* 123 (2001)
503 503–518.
- 504 [15] K. Sudarshan, P.J. Paul, H.S. Mukunda, *Proc.*
505 *Combust. Inst.* 29 (2002) 1131–1137.
- 506 [16] M. de Joannon, G. Langella, F. Beretta, A. Cav-
507 aliere, C. Noviello, *Proc. Mediterr. Combust. Sym-*
508 *pos.* 3 (1999) 347–360.
- [17] A. Milani, A. Saponaro, *Diluted combustion* 509
technologies, IFRF Combust. J. Article 200101
(2001).
- [18] R. Weber, S. Orsino, L. Nicolas, A. Verlaan, *Proc.* 512
Combust. Inst. 28 (2000) 1315–1321.
- [19] M. Mancini, R. Weber, U. Bollettini, *Proc. Com-* 514
combust. Inst. 29 (2002) 1155–1164.
- [20] S. Lille, T. Dobski, W. Blasiak, *J. Propuls. Power* 516
16 (4) (2000) 595–600.
- [21] H.S. Mukunda, S. Dasappa, U. Shrinivasa, in: T.B.
518 Johansson, H. Kelly (Eds.), *Renewable Energy–*
Sources for Fuels and Electricity, Island press,
Washington, DC, 1993, pp. 699–728.
- [22] ABETS, *Biomass to Energy—The Science and* 522
Technology of the IISc Bio-energy systems. ABETS,
Indian Institute of Science Bangalore, India. 525